MULTI-TYPE SENSOR PLACEMENT AND DATA FUSION FOR STRUCTURAL MONITORING: NUMERICAL SIMULATION

X. H. Zhang [1], S. Zhu [2] and Y. L. Xu [2]
[1] Department of Civil and Structural Engineering,
The Hong Kong Polytechnic University, China. Email: xh.zhang@polyu.edu.hk
[2] Department of Civil and Structural Engineering, The Hong Kong Polytechnic University, China.

ABSTRACT

Nowadays structural health monitoring systems (SHMS) play important roles in assuring the serviceability and safety of some critical infrastructures during their long service lives. The operational performance of SHMS substantially relies on the features of sensor system, including types, number and spatial allocation in structures. Since the number of sensors is always limited compared with degrees-of-freedom of a large-scale structure, the determination of sensor number and locations becomes a critical issue encountered in the design and implementation of an effective SHMS. Meanwhile, the fast development of sensor technology makes various types of sensors available for structural health monitoring purpose, enabling the monitoring of both global behavior and local response. Even though such comprehensive SHMS have been instrumented in many newly-built critical structures, surprisingly little work in the literature focuses on the optimal design of global and local sensors for structural health monitoring. Therefore, this paper attempts to addresses this knowledge gap—the location selection and data fusion of a multi-type sensor system in a structure including displacement transducers, accelerometers and strain gauges, all of which are commonly used in SHMS. The number and locations of the three types of sensors are optimized with the objective of minimizing the estimation error of unobserved structural responses based on incomplete measurement. Unlike traditional approaches for sensor placement in which each type sensors are designed separately, this study designs the whole sensor system simultaneously. By minimizing the overall estimation errors at the locations of interest and reducing estimation errors to a desired target level, the initial set of candidate sensor locations is reduced to a smaller optimal set. Kalman filter algorithm is employed in the sensor placement and data fusion. A numerical examples—a two-dimensional truss structure—was presented to illustrate the effectiveness and accuracy of the proposed approach for the location selection and data fusion of multi-type sensors.

KEYWORDS

Structural monitoring, Multi-type sensor placement, Kalman filter algorithm, Estimation, Numerical simulation.

INTRODUCTION

In the past two decades, quite a few important structures have established the comprehensive structural health monitoring systems (SHMS) which has become a trend with the utmost goals of ensuring the functionality and safety of the structures during their long service life. The operational performance of SHMS substantially relies on the features of the sensor system such as the type, number, spatial location and signal quality. Meanwhile, with the fast development of sensor technology, various types of sensors are now available to measure not only the global but also the local response or features of the structure, both of which are important to SHMS. It is impractical to install sensors on every part of a structure, especially for a large-scale structure. Therefore, there arise two critical issues in the implementation of an effective SHMS, (1) optimal location selection and data fusion of multi-type sensors; (2) estimation of unmeasured response based on measurements at limited locations.

Numerous techniques have been developed over the past decades on solving the problem of optimal sensor placement for the purpose of parameter identification, structural control and structural health monitoring. To provide maximum information on the state of structures, a class of information based approaches has been extensively studied by some researches, for example, Effective Independence (EfI) method (Kammer 1991), Effective Independence-Drive point residue (EfI-DPR) method (Imamovic 1998), Variance method (Meo and Zumpano 2005) and information entropy method (Paradinitriou et al., 2000). Meo and Zumpano compared the variance method with other five methods in their study, concluding that the EfI-DPR method provides an

effective way for optimal sensor placement to identify the low frequency vibration characteristics. Another class of sensor optimal placement method is energy based method (Hemez and Farhat 1994; Heo et al. 1997). Further examples of energy based sensor placement method include the eigenvalue vector product (Jarvis, 1991) and non-optimal drive point (Imamovic, 1998) methods. Lim (1992) employed a function of the system controllability and observability to develop a sensor placement approach. Another method called modal assurance criterion (MAC) based method was presented by Carne and Dohrmann (1995) to attain the sensor configuration by minimizing the off-diagonal terms in the MAC matrix. Beal et al. (2008) formulated optimal sensor placement as a mixed variable programming (MVP) problem. In addition to the above-mentioned examples, many other sensor placement approaches exist in the literature, and a good review is provided by Barthorpe and Worden (2009). Most existing approaches are intended for system identification or damage detection based on single-type sensor system. So far very few attentions have been paid to the estimation of unmeasured response with a multi-type sensor system. As a well-known state estimator algorithm, Kalman filter has found wide applications in data fusion problems (Bar-Shalom and Li 1995). Two common examples are Kalman filter based measurement fusion and state fusion (Gao and Harris 2002). Kalman filter has also been applied by some researchers in chemical fields to select sensor locations of multi-types (Amaya and Aoki 1999; Musulin et al. 2005). However, the complex structures in civil engineering field may bring more challenges to multi-type sensor locations selection and data fusion.

This paper investigates a practical and challenging problem how to place multi-type sensors, including strain gauges, displacement transducers, and accelerometers which are common used in SHMS, so that both local and global monitoring information can be best integrated for structural health evaluation. The objective is to locate a small number of sensors that yield a good estimation of the structural response. The number and locations of the three type sensors are determined aiming to minimize the estimation errors of unobserved structural responses using limited measurements and Kalman filter algorithm. It should be noted that conventionally the spatial configurations of multi-type sensors are designed in separate and distinct processes, while in this study the design of the multi-type sensor system is performed simultaneously, and the measurements from three types of sensors are fused together to estimate the response of entire structure. The posteriori error covariance is selected as a performance measure for assessing the estimation accuracy in the optimization process. A case study of a two-dimensional truss structure is presented as an example. The results of the numerical analysis indicate that the proposed approach offers an effective way to design a multi-type sensor system and the optimal sensor locations can produce the estimation of actual response with sufficient accuracy.

SENSOR PLACEMENT

Multi-type Sensor Data Fusion

Based on the finite element representation of a structure, the equations of motions are given by

$$\mathbf{M}\ddot{\mathbf{x}} + \mathbf{C}_d\dot{\mathbf{x}} + \mathbf{K}\mathbf{x} = \mathbf{B}_u\mathbf{u} \tag{1}$$

in which $\mathbf{M}$, $\mathbf{C}_d$, and $\mathbf{K}$ are the mass, damping and stiffness matrices, respectively, $\mathbf{B}_u$ is the location matrix of excitations, and $\mathbf{u}$ is external excitation vector. Eq. (1) can be rewritten with regard to the modal coordinates $\mathbf{q}$.

$$\ddot{\mathbf{q}} + 2\xi\boldsymbol{\omega}_o\dot{\mathbf{q}} + \boldsymbol{\omega}_o^2\mathbf{q} = \boldsymbol{\Phi}^T\mathbf{B}_u\mathbf{u} \tag{2}$$

where $\mathbf{q}$ is the vector of modal coordinates; $\boldsymbol{\Phi}$ is mass normalized vibration mode shapes obtained from finite element model; ξ is modal damping coefficient matrix; $\boldsymbol{\omega}_o$ is modal frequency matrix. In practice, only a small number of vibration modes, often much less the total DOFs of a complex structure, play important roles in structural dynamic response. Eq. (2) is in a greatly reduced-order compared with Eq. (1) and it can be further transformed to a state-space form

$$\dot{\mathbf{z}} = \mathbf{A}_c\mathbf{z} + \mathbf{B}_c\mathbf{u} \tag{3}$$

where

$$\mathbf{z} = \begin{Bmatrix}\mathbf{q}\\ \dot{\mathbf{q}}\end{Bmatrix};\ \mathbf{A}_c = \begin{bmatrix}\mathbf{0} & \mathbf{I}\\ -\boldsymbol{\omega}_o^2 & -2\xi\boldsymbol{\omega}_o\end{bmatrix};\ \mathbf{B}_c = \begin{bmatrix}\mathbf{0}\\ \boldsymbol{\Phi}^T\mathbf{B}_u\end{bmatrix} \tag{4}$$

For a linear structural system, the corresponding general sensor response can be expressed as a linear combination of the state and input

$$\mathbf{y} = \mathbf{C}\mathbf{z} + \mathbf{D}\mathbf{u} \tag{5}$$

Assume that the response vector $\mathbf{y}$ includes the displacements, strains, and accelerations at the locations of interest. In this study, the measurement vector monitored by the three types of sensors are directly merged into a

new measurement vector, i.e. $\mathbf{y} = \begin{bmatrix} \boldsymbol{\varepsilon} & \mathbf{d} & \mathbf{a} \end{bmatrix}^T$, where **ε**, **d** and **a** represent strain, displacement and acceleration responses respectively. Then the measurement equation has the following form

$$\mathbf{y} = \begin{Bmatrix} \boldsymbol{\varepsilon} \\ \mathbf{d} \\ \mathbf{a} \end{Bmatrix} = \begin{bmatrix} \boldsymbol{\Psi} & 0 \\ \boldsymbol{\Phi} & 0 \\ -\boldsymbol{\Phi}\boldsymbol{\omega}_o^2 & -2\boldsymbol{\Phi}\boldsymbol{\xi}\boldsymbol{\omega}_o \end{bmatrix} \mathbf{z} + \begin{bmatrix} 0 \\ 0 \\ \boldsymbol{\Phi}\boldsymbol{\Phi}^T\mathbf{B}_u \end{bmatrix} \mathbf{u} = \mathbf{C}\mathbf{z} + \mathbf{D}\mathbf{u} \tag{6}$$

where $\boldsymbol{\Psi}$ denotes strain mode shapes. In reality, the measurements will be sampled at discrete instants with a sample period of Δt. Moreover, sensor noise always influences the sample data practically. Therefore, after sampling the state space model in a discrete form is

$$\begin{cases} \mathbf{z}_{k+1} = \mathbf{A}\mathbf{z}_k + \mathbf{B}\mathbf{u}_k + w_k \\ \mathbf{y}_k = \mathbf{C}\mathbf{z}_k + \mathbf{D}\mathbf{u}_k + v_k \end{cases} \tag{7}$$

where $\mathbf{z}_k = \mathbf{z}(k\Delta t)$ is the discrete time state vector ($k \in \mathbf{N}$); $\mathbf{A} = e^{\mathbf{A}_c \Delta t}$ is the discrete state matrix; $\mathbf{B} = \int_0^{\Delta t} e^{\mathbf{A}_c \tau'} d\tau' \mathbf{B}_c$ denotes the discrete input matrix; $\mathbf{w}_k$ is the process noise duo to disturbances and modeling inaccuracies, often assumed as a white noise with zero mean and a variance **Q; C** represents the direct output matrix; **D** is called the direct transmission matrix; $\mathbf{v}_k$ is the measurement noise due to sensor inaccuracy with a variance **R.** It is common to assume that sensors of the same types have equal noise variances.

Kalman Filter Algorithm

The Kalman filter gives an unbiased, minimum error and recursive algorithm to optimally estimate the unknown state of a linear dynamic system from observations with Gaussian white noise. Suppose that n_m sensor locations are chosen, $n_m = n^{\varepsilon}_m + n^{d}_m + n^{a}_m$, where the subscript '*m*' denotes the measurement, and n^{ε}_m, n^{d}_m and n^{a}_m denote the number of strain gauges, displacement transducers and accelerometers respectively. From Eq. (7), the discrete state-space dynamic model and measurement model has the following form

$$\begin{cases} \mathbf{z}_{k+1} = \mathbf{A}\mathbf{z}_k + \mathbf{B}\mathbf{u}_k + w_k \\ \mathbf{y}_k = \mathbf{C}_m\mathbf{z}_k + \mathbf{D}_m\mathbf{u}_k + v_k \end{cases} \tag{8}$$

where matrix $\mathbf{C}_m$ and $\mathbf{D}_m$ is the output matrix and the direct transmission matrix respectively corresponding to the positions with sensors.

The Kalman filter equations are divided into two groups: time update equations and measurement update equations (Welch and Bishop 2001):

Time update equations

$$\hat{\mathbf{z}}_{k|k-1} = \mathbf{A}\hat{\mathbf{z}}_{k-1|k-1} + \mathbf{B}u_{k-1} \tag{9}$$

$$\mathbf{P}_{k|k-1} = \mathbf{A}\mathbf{P}_{k-1|k-1}\mathbf{A}^{\mathbf{T}} + \mathbf{Q} \tag{10}$$

Measurement update equations

$$\hat{\mathbf{z}}_{k|k} = \hat{\mathbf{z}}_{k|k-1} + \mathbf{K}_k[\mathbf{y}_k - \mathbf{C}_m\hat{\mathbf{z}}_{k|k-1} - \mathbf{D}u_k] \tag{11}$$

$$\mathbf{P}_{k|k} = [\mathbf{I} - \mathbf{K}_k\mathbf{C}_m]\mathbf{P}_{k|k-1} \tag{12}$$

where Kalman gain $\mathbf{K}_k$ is the optimal gain given by

$$\mathbf{K}_k = \mathbf{P}_{k|k-1}\mathbf{C}_m^T[\mathbf{C}_m\mathbf{P}_{k|k-1}\mathbf{C}_m^T + \mathbf{R}_m]^{-1} \tag{13}$$

$\mathbf{R}_m$ is the covariance matrix of the measurement noise which has similar format but different dimensions with **R**. It should be pointed out that the output influence matrix **C** tends to be highly ill-conditioned because the strain, the displacement and the acceleration have different orders of magnitude. The inverse operation in Eq. (13) may result in inaccuracy. The standard deviation of sensor noise is proposed by Zhang et al. (2011) to normalize the output matrix **C**

$$\widetilde{\mathbf{C}} = \begin{bmatrix} \dfrac{\boldsymbol{\Psi}}{\sigma_\varepsilon} & 0 \\ \dfrac{\boldsymbol{\Phi}}{\sigma_d} & 0 \\ \dfrac{-\boldsymbol{\Phi}\boldsymbol{\omega}_o^2}{\sigma_a} & \dfrac{-2\boldsymbol{\Phi}\boldsymbol{\xi}\boldsymbol{\omega}_o}{\sigma_a} \end{bmatrix} = \mathbf{R}^{-\frac{1}{2}}\mathbf{C} \tag{14}$$

where,

$$\mathbf{R} = E(vv^{\mathrm{T}}) = \begin{bmatrix} \sigma_\varepsilon^2\mathbf{I} & & \\ & \sigma_d^2\mathbf{I} & \\ & & \sigma_a^2\mathbf{I} \end{bmatrix} \tag{15}$$

in which σ_ε^2, σ_d^2 and σ_a^2 are the noise variance, the subscripts '*s*', '*d*' and '*a*' stand for 'strain gauges' ,'displacement transducers' and 'accelerometers' respectively, and $\mathbf{I}$ is the identity matrix. Thus, the optimal Kalman gain can be rewritten as

$$\mathbf{K}_k = \mathbf{P}_{k|k-1}\widetilde{\mathbf{C}}_m^T[\widetilde{\mathbf{C}}_m\mathbf{P}_{k|k-1}\widetilde{\mathbf{C}}_m^T + \mathbf{I}]^{-1}\mathbf{R}_m^{-\frac{1}{2}} \tag{16}$$

$\mathbf{P}_{k|k}$ is the covariance matrix of the state vector estimation error. Usually the Kalman filter converges in the iterations, given any initial conditions $\mathbf{P}_0$ and $\hat{\mathbf{z}}_0$. The asymptotic value of $\mathbf{P}_{k|k}$ is considered as a stable indication of estimation accuracy

$$\mathbf{P} = \lim_{k\to t}([\mathbf{P}_{k|k}]) \tag{17}$$

In this study, the estimation of the structural response is of interest, which can be computed based on the unbiased estimated state vector.

$$\mathbf{y}_e = \begin{Bmatrix} \boldsymbol{\varepsilon}_e \\ \mathbf{d}_e \\ \mathbf{a}_e \end{Bmatrix} = \begin{bmatrix} \boldsymbol{\Psi} & 0 \\ \boldsymbol{\Phi} & 0 \\ -\boldsymbol{\Phi}\boldsymbol{\omega}_o^2 & -2\boldsymbol{\Phi}\boldsymbol{\xi}\boldsymbol{\omega}_o \end{bmatrix}\hat{\mathbf{z}} + \begin{bmatrix} 0 \\ 0 \\ \boldsymbol{\Phi}\boldsymbol{\Phi}^T\mathbf{B}_u \end{bmatrix}\mathbf{u} = \mathbf{C}\hat{\mathbf{z}} + \mathbf{D}\mathbf{u} \tag{18}$$

Thereby, the estimation error covariance of $\mathbf{y}_e$ is given by,

$$\begin{aligned} \Delta &= \mathrm{cov}(\mathbf{y}_e - \mathbf{y}) = \mathrm{cov}(\mathbf{C}\hat{\mathbf{z}} + \mathbf{D}\mathbf{u} - \mathbf{C}\mathbf{z} - \mathbf{D}\mathbf{u}) \\ &= \mathrm{cov}(\mathbf{C}\hat{\mathbf{z}} - \mathbf{C}\mathbf{z}) = \mathbf{C}\,\mathrm{cov}(\hat{\mathbf{z}} - \mathbf{z})\mathbf{C}^T = \mathbf{C}\mathbf{P}\mathbf{C}^T \end{aligned} \tag{19}$$

in which $\mathbf{y}_e = [\boldsymbol{\varepsilon}_e \quad \mathbf{d}_e \quad \mathbf{a}_e]^T$ is the estimated response vectors.

Sensor Placement

Each diagonal element of $\boldsymbol{\Delta}$ matrix represents the variance of the estimation error for corresponding response (strain, displacement or accelerometer). Therefore, the maximum diagonal element denotes the maximum estimation error, while the trace of the matrix $\boldsymbol{\Delta}$ represents the sum of estimation errors at all locations of interest. The optimal sensor placement can be performed by minimizing the estimation error. However, the magnitudes of strain, displacement and acceleration response are of different orders, and so are their absolute estimation errors. As pointed out by Zhang et al. (2011), the optimization procedure may considerably bias one type of sensors without a proper normalization. In light of this, the relative estimation error is used

$$\widetilde{\boldsymbol{\delta}} = \mathbf{R}^{-\frac{1}{2}}(\mathbf{y}_e - \mathbf{y}) = \begin{bmatrix} \dfrac{(\boldsymbol{\varepsilon}_e - \boldsymbol{\varepsilon})}{\sigma_\varepsilon} & \dfrac{(\mathbf{d}_e - \mathbf{d})}{\sigma_d} & \dfrac{(\mathbf{a}_e - \mathbf{a})}{\sigma_a} \end{bmatrix}^T \tag{20}$$

The noise-normalized estimated response error covariance can be computed by

$$\widetilde{\Delta} = \mathrm{cov}(\widetilde{\boldsymbol{\delta}}) = \widetilde{\mathbf{C}}\mathbf{P}\widetilde{\mathbf{C}}^T \tag{21}$$

The maximum and average estimation errors at all locations yields

$$\widetilde{\sigma}_{\max}^2 = \max(diag(\widetilde{\Delta})) \tag{22}$$

$$\tilde{\sigma}_{avg}^2 = \frac{tr(\tilde{\Delta})}{n} = \frac{tr[\tilde{\mathbf{C}}\mathbf{P}\tilde{\mathbf{C}}^T]}{n} \tag{23}$$

The objective function and constraint function of the sensor location selection can be written as

$$\min\ \tilde{\sigma}_{avg}^2 \Rightarrow \min\ tr[\tilde{\mathbf{C}}\mathbf{P}\tilde{\mathbf{C}}^T] \tag{23}$$

subject to

$$\tilde{\sigma}_{\max}^2 \le \left[\tilde{\sigma}_{\max}^2\right],\ \tilde{\sigma}_{avg}^2 \le \left[\tilde{\sigma}_{avg}^2\right] \tag{24}$$

in which $[\tilde{\sigma}_{\max}^2]$ and $[\tilde{\sigma}_{avg}^2]$ are the target normalized maximum and average estimated errors respectively. During the optimization procedure, the maximum and average estimation errors will be increased with the reduction of the number of sensors. The candidate sensor positions are removed one by one, until the prescribed criterion for estimation errors is achieved (as shown in constraint functions). A simple iterative procedure is carried out, in which the candidate sensor positions are deleted one by one until the target error level is reached. In each step, one sensor location is removed which results in a minimal trace of the matrix $(\tilde{\mathbf{C}}\mathbf{P}\tilde{\mathbf{C}}^T)$. Once the sensor locations are selected, the response at other locations can be estimated using Eq. (18). It should be noted that such a simple procedure can be only applied to relative simple structures. For large-scale or complex structures with a large number of DOFs, this procedure is time-consuming and possibly suboptimal. Some common optimization methods, e.g. genetic algorithm, could be employed in that case.

NUMERICAL SIMULATION

The processes of sensor location selection and responses estimation are demonstrated using a two-dimensional truss structure shown in Figure 1(a). The finite element model consists of 25 elements, 14 nodes and 28 degrees of freedom. The members are connected at pinned joints each with two degrees of freedom. A random excitation is applied vertically at the node 4, and it induces the flexural vibration of the truss. It should be pointed out that the proposed approach is suitable for any types of excitation. The random force is adopted only for the purpose of illustration; because the random force is widely used to represent a general load civil engineering structures subject to its corresponding response may involve more vibration modes than harmonic excitation or free vibration. The deformation of each element, the displacement and acceleration of each node are of interest in this study. Considering that it is not easy to measure the rotations at nodes in practice, rotational degrees of freedom are eliminated in the concerned mode shapes. The strain gauges are attached to the upper face at the middle of the elements to measure the flexural deformation of the beam. As a result, 25 element strains, 12 vertical nodal displacements, 13 transversal nodal displacements, 12 vertical nodal accelerations and 13 transversal nodal accelerations are identified as the response of interest, and they are also taken as the candidate locations for sensors. In practice, however, the sensor installment may be restricted by the approachability of each location. Meanwhile, strain gauges are supposed to be attached away from the location with stress concentration, although those locations are also hot-spots of great interest in real applications

In this study, the noise variances are assumed to be constant for each type of sensors, and they are independent with magnitude of response signals. In reality, sensor noise level depends not only on the type of sensors, but also on the environment and instrumentations. Hence some site-specific empirical values should be taken for sensor noise variances. In this study, σ_ε =0.08uε, σ_d =0.002mm and σ_a =0.29m/s^{-2}.

The first six mode shapes are considered in this case study, and the contribution of higher modes is assumed negligible. The proposed approach is adopted to optimize the locations of strain gauges, displacement transducers and accelerometers simultaneously, and the total number of sensors is determined based on the constraints of $\tilde{\sigma}_{\max}^2 \le 1.0$ and $\tilde{\sigma}_{avg}^2 \le 0.5$. Figure 2 depicts the variation of the average and maximum normalized estimation error variance in the optimization procedure, i.e. $\tilde{\sigma}_{avg}^2$ and $\tilde{\sigma}_{\max}^2$. The sensor location which contributes most to minimize the trace of the error variance matrix $\tilde{\mathbf{\Lambda}}$ is removed from the candidate locations in each step. Both $\tilde{\sigma}_{\max}^2$ and $\tilde{\sigma}_{avg}^2$ become larger with the decrease of the sensor number. Therefore, the final sensor number is determined when the aforementioned criteria are reached. As a results, totally 10 sensors are selected, comprising of four strain gauges, one displacement transducers in y-direction, and five accelerometers in y-direction, and their corresponding optimal locations are shown in Figure 1(b).

The response data contaminated by noises from the optimal multi-type sensor are employed to estimate the responses at remaining locations using Eq. 18. It should be noted that the Kalman filter gain is computed from

Eq. 16 to avoid the ill-condition inverse problem. Figures 3-5 illustrates the comparison of the estimated response and the real response of strain at element 7, element 12, element 23, the vertical response of displacement and acceleration at node 4, node 10 and node 14, respectively. As displayed in Figures, the estimated strain, displacement and acceleration can match the real response fairly well.

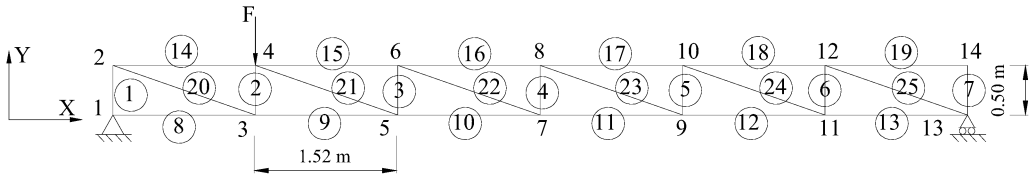

(a) 25-Bar truss structure

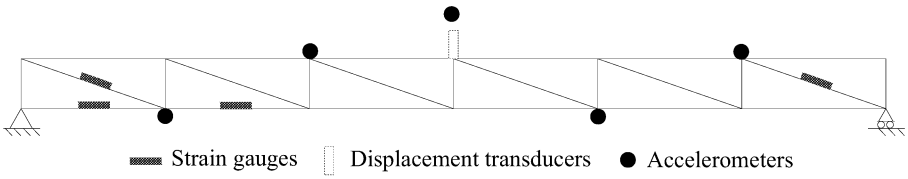

(b) Selected sensor locations

Figure 1 Finite element model and sensor locations

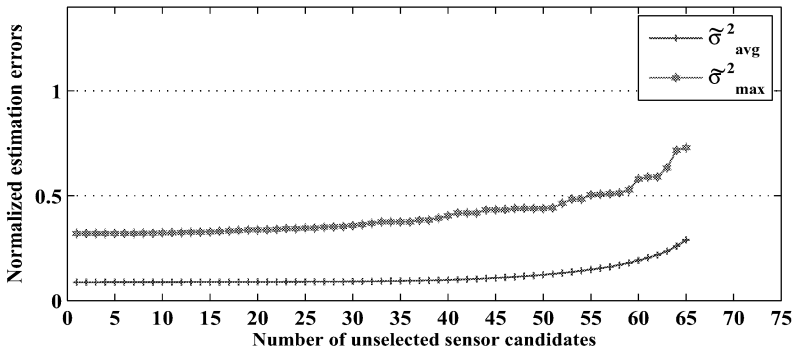

Figure 2 Variation of theoretical estimation errors with number of sensors

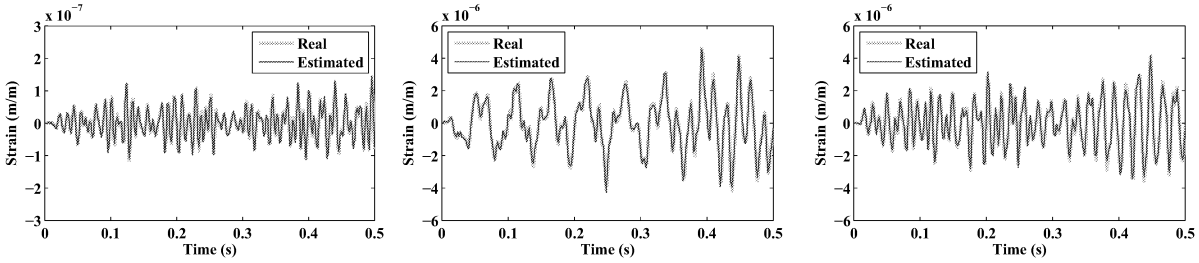

(a) Element 7 (b) Element 12 (c) Element 23

Figure 3 Strain time history responses

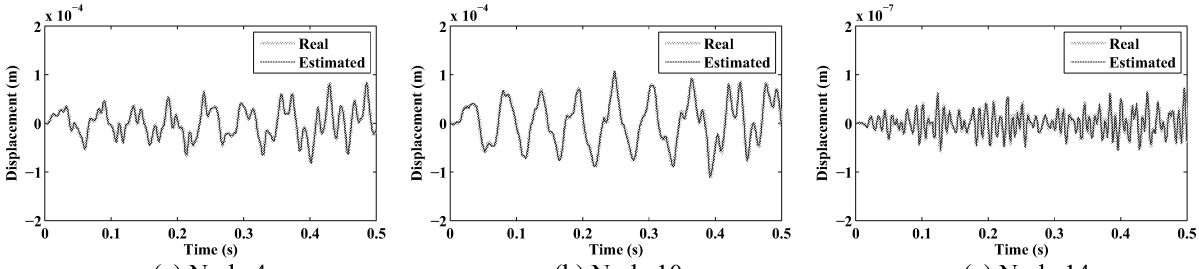

(a) Node 4 (b) Node 10 (c) Node 14

Figure 4 Displacement time history responses

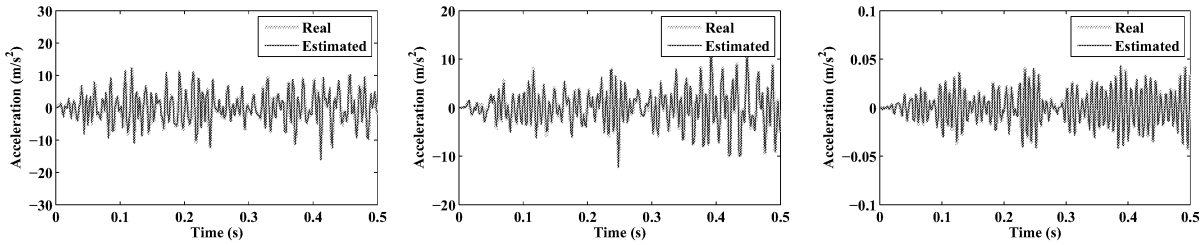

(a) Node 4 (b) Node 10 (c) Node 14

Figure 5 Acceleration time history responses

The errors in the estimated results is defined as the relative percentage error (RPE) between the estimated response and the real response,

$$RPE = \frac{std(\mathbf{y}_e - \mathbf{y}_m)}{std(\mathbf{y}_m)} \times 100\% \tag{24}$$

where "*std*" means the standard deviation, $\mathbf{y}_e$ and $\mathbf{y}_m$ are the estimated and measured time histories respectively. Figure 6 shows the relative percentage errors (RPEs) in the estimated results at the corresponding components. It can be found from the figure that the estimated results are quite accurate and most of the RPEs are below 10%, except those near the excitation location or near the support locations. This is because the responses near these locations are much more complex and the responses near the support location are small than others.

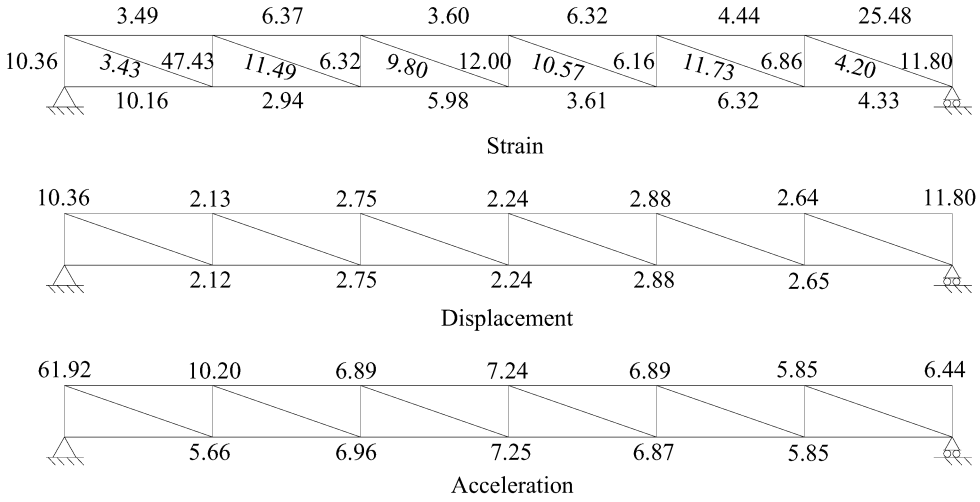

Figure 6 Relative percentage errors

CONCLUSIONS

A multi-type sensor location selection approach is presented for structural monitoring systems consisting of strain gauges, displacement transducers and accelerometers. The locations of multi-type sensors are selected simultaneously in this approach instead of being carried out in separate courses. The location optimization objective is to best estimate the key structural response and the total number of sensors is determined to achieve the desired error levels in structural response estimations. Noise-normalized responses and mode shapes are used in this approach. Subsequently, the measurements from the limited three types of sensors are employed collectively to estimate the response of the entire structure by using the Kalman filter algorithm. A numerical analysis of a two-dimensional truss structure indicates that this approach offers an effective way to design such a multi-type sensor system as a whole and the measurement from the limited locations can predict structural response with sufficient accuracy.

REFERENCES

Amaya K and Aoki S (1999). Optimization of measurements for inverse problem. *Proceedings of the third International Conference on Inverse Problems in Engineering*, June 13-18, Port Ludlow, WA, USA, 1-6.

Bar-Shalom Y and Li X (1995). *Multitarget–Multisensor Tracking: Principles and Techniques*. YBS Publishing, Storrs, CT.

Barthorpe RJ and Worden K (2009). Sensor placement optimization. *Encyclopedia of Structural Health Monitoring*, John Wiley & Sons, Ltd, 1239-1250.

Beal, J.M., Shukla, A., Brezhneva, O.A., and Abramson, M.A. (2008), Optimal sensor placement for enhancing sensitivity to change in stiffness for structural health monitoring, *Optimization and Engineering*, 9(2), 119-142.

Carne, T.G. and Dohrmann, C.R. (1995), A modal test design strategy for model correlation, *Proceedings of the 13th International Modal Analysis Conference*, Nashville, TN.

Gao JB and Harris CJ (2002). Some remarks on Kalman filters for the multisensor fusion. *Information fusion*, 3, 191-201.

Hemez FM and Farhat C (1994). An energy based optimum sensor placement criterion and its application to structure damage detection. *Proceedings of the 12th International Conference on Modal Analysis, Society of Experimental Mechanics*, Honolulu, 1568–1575.

Heo G, Wang ML and Satpathi D (1997). Optimal transducer placement for health monitoring of long span bridge. *Soil Dynamics and Earthquake Engineering*. 16, 495–502.

Imamovic N (1998). *Model validation of large finite element model using test data*. Ph.D. thesis, Imperial college London.

Jarvis, B. (1991), Enhancements to modal testing using finite elements, *Journal of Sound and Vibration*, 25(8), 28-30.

Kammer DC (1991). Sensor placement for on-orbit modal identification and correlation of large space structures. *Journal of Guidance, Control and Dynamics*. 14(2), 251-259.

Lim, K.B. (1992), Method for optimal actuator and sensor placement for large flexible structures, *Journal of Guidance, Control and Dynamics*, 15, 49–57.

Meo M and Zumpano G (2005). On the Optimal Sensor Placement Techniques for a Bridge Structure. *Engineering Structures*. 27, 1488 – 1497.

Musulin E, Benqlilou C, Bagajewicz MJ and Puigjaner L (2005). Instrumentation design based on optimal Kalman filtering, *Journal of Process Control*. 15, 629-638.

Papadimitriou, C., Beck, J.L. and Au, S.K. (2000), Entropy-based optimal sensor location for structural model updating, *Journal of Vibration and Control*, 6, 781-800.

Welch G and Bishop G (2001). *An introduction to the Kalman filter. Technical report*. University of North Carolina, Chapel Hill, NC, USA.

Zhang XH, Zhu S, Xu YL and Hong XJ (2011). Integrated optimal placement of displacement transducers and strain gauges for better estimation of structural response, *International Journal of Structural Stability and Dynamics*, 11(3), 1-22.